EXPLAINING EXTREME EVENTS OF 2016

From A Climate Perspective

Special Supplement to the
Bulletin of the American Meteorological Society
Vol. 99, No. 1, January 2018

EXPLAINING EXTREME EVENTS OF 2016 FROM A CLIMATE PERSPECTIVE

Editors

Stephanie C. Herring, Nikolaos Christidis, Andrew Hoell, James P. Kossin,
Carl J. Schreck III, and Peter A. Stott

Special Supplement to the

Bulletin of the American Meteorological Society

Vol. 99, No. 1, January 2018

American Meteorological Society

Corresponding Editor:

Stephanie C. Herring, PhD
NOAA National Centers for Environmental Information
325 Broadway, E/CC23, Rm 1B-131
Boulder, CO 80305-3328
E-mail: stephanie.herring@noaa.gov

Cover credit:

©The Ocean Agency / XL Catlin Seaview Survey / Chrisophe Bailhache—A panoramic image of coral bleaching at Lizard Island on the Great Barrier Reef, captured by The Ocean Agency / XL Catlin Seaview Survey / Christophe Bailhache in March 2016.

HOW TO CITE THIS DOCUMENT

Citing the complete report:

Herring, S. C., N. Christidis, A. Hoell, J. P. Kossin, C. J. Schreck III, and P. A. Stott, Eds., 2018: Explaining Extreme Events of 2016 from a Climate Perspective. *Bull. Amer. Meteor. Soc.*, **99** (1), S1–S157.

Citing a section (example):

Quan, X.W., M. Hoerling, L. Smith, J. Perlwitz, T. Zhang, A. Hoell, K. Wolter, and J. Eischeid, 2018: Extreme California Rains During Winter 2015/16: A Change in El Niño Teleconnection? [in "Explaining Extreme Events of 2016 from a Climate Perspective"]. *Bull. Amer. Meteor. Soc.*, **99** (1), S54–S59, doi:10.1175/BAMS-D-17-0118.1.

EDITORIAL AND PRODUCTION TEAM

Riddle, Deborah B., Lead Graphics Production, NOAA/NESDIS National Centers for Environmental Information, Asheville, NC

Love-Brotak, S. Elizabeth, Graphics Support, NOAA/NESDIS National Centers for Environmental Information, Asheville, NC

Veasey, Sara W., Visual Communications Team Lead, NOAA/NESDIS National Centers for Environmental Information, Asheville, NC

Fulford, Jennifer, Editorial Support, Telesolv Consulting LLC, NOAA/NESDIS National Centers for Environmental Information, Asheville, NC

Griffin, Jessicca, Graphics Support, Cooperative Institute for Climate and Satellites-NC, North Carolina State University, Asheville, NC

Misch, Deborah J., Graphics Support, Telesolv Consulting LLC, NOAA/NESDIS National Centers for Environmental Information, Asheville, NC

Osborne, Susan, Editorial Support, Telesolv Consulting LLC, NOAA/NESDIS National Centers for Environmental Information, Asheville, NC

Sprain, Mara, Editorial Support, LAC Group, NOAA/NESDIS National Centers for Environmental Information, Asheville, NC

Young, Teresa, Graphics Support, Telesolv Consulting LLC, NOAA/NESDIS National Centers for Environmental Information, Asheville, NC

TABLE OF CONTENTS

ABSTRACT—Stephanie C. Herring, Nikolaos Christidi, Andrew Hoell, James P. Kossin, Carl J. Schreck III, and Peter A. Stott

This sixth edition of explaining extreme events of the previous year (2016) from a climate perspective is the first of these reports to find that some extreme events were not possible in a preindustrial climate. The events were the 2016 record global heat, the heat across Asia, as well as a marine heat wave off the coast of Alaska. While these results are novel, they were not unexpected. Climate attribution scientists have been predicting that eventually the influence of human-caused climate change would become sufficiently strong as to push events beyond the bounds of natural variability alone. It was also predicted that we would first observe this phenomenon for heat events where the climate change influence is most pronounced. Additional retrospective analysis will reveal if, in fact, these are the first events of their kind or were simply some of the first to be discovered.

Last year, the editors emphasized the need for additional papers in the area of "impacts attribution" that investigate whether climate change's influence on the extreme event can subsequently be directly tied to a change in risk of the socio-economic or environmental impacts. Several papers in this year's report address this challenge, including Great Barrier Reef bleaching, living marine resources in the Pacific, and ecosystem productivity on the Iberian Peninsula. This is an increase over the number of impact attribution papers than in the past, and are hopefully a sign that research in this area will continue to expand in the future.

Other extreme weather event types in this year's edition include ocean heat waves, forest fires, snow storms, and frost, as well as heavy precipitation, drought, and extreme heat and cold events over land. There were a number of marine heat waves examined in this year's report, and all but one found a role for climate change in increasing the severity of the events. While human-caused climate change caused China's cold winter to be less likely, it did not influence U.S. storm Jonas which hit the mid-Atlantic in winter 2016.

As in past years, the papers submitted to this report are selected prior to knowing the final results of whether human-caused climate change influenced the event. The editors have and will continue to support the publication of papers that find no role for human-caused climate change because of their scientific value in both assessing attribution methodologies and in enhancing our understanding of how climate change is, and is not, impacting extremes. In this report, twenty-one of the twenty-seven papers in this edition identified climate change as a significant driver of an event, while six did not. Of the 131 papers now examined in this report over the last six years, approximately 65% have identified a role for climate change, while about 35% have not found an appreciable effect.

Looking ahead, we hope to continue to see improvements in how we assess the influence of human-induced climate change on extremes and the continued inclusion of stakeholder needs to inform the growth of the field and how the results can be applied in decision making. While it represents a considerable challenge to provide robust results that are clearly communicated for stakeholders to use as part of their decision-making processes, these annual reports are increasingly showing their potential to help meet such growing needs.

16. WARM WINTER, WET SPRING, AND AN EXTREME RESPONSE IN ECOSYSTEM FUNCTIONING ON THE IBERIAN PENINSULA

Sebastian Sippel*, Tarek S. El-Madany*, Mirco Migliavacca, Miguel D. Mahecha, Arnaud Carrara, Milan Flach, Thomas Kaminski, Friederike E. L. Otto, Kirsten Thonicke, Michael Vossbeck, and Markus Reichstein

A warm winter 2015/16 followed by a wet spring enabled exceptionally high ecosystem gross primary productivity on the Iberian Peninsula. Climate-ecosystem model simulations show warming winters and increased CO_2 availability benefit ecosystem productivity, but no increase in spring precipitation.

Introduction. The Iberian Peninsula (IP) experienced unusual meteorological conditions in winter and spring 2015/16 (WS15/16) with a warm winter followed by wet conditions in late winter and spring (Figs. 16.1a–c). The unusual succession of these events coincided with an extremely positive anomaly in vegetation productivity on local and regional scales over the IP with unusually high regional vegetation greenness (Figs. 16.1d–f; a proxy for ecosystem productivity) and high crop yields (JRC MARS Bulletins 2016, https://ec.europa.eu/jrc/en/research-topic/crop-yield-forecasting).

Climatic changes can affect the intensity and frequency of extreme events (Seneviratne et al. 2012), and these changes are widely recognized to impose substantial impacts on terrestrial ecosystems (Reichstein et al. 2013). However, interpreting and quantifying climate-induced ecosystem impacts such as the vegetation productivity on the IP in WS15/16 remains challenging as continuous site-level measurements that span over a decade are generally rare, and even the longest site measurements are only available for the last 25 years (http://fluxnet.fluxdata.org/data/fluxnet2015-dataset/).

AFFILIATIONS: Sippel—Max Planck Institute for Biogeochemistry, Jena, Germany, and now at Norwegian Institute of Bioeconomy Research (NIBIO), Ås, Norway; El-Madany, Migliavacca, Mahecha, Flach, and Reichstein—Max Planck Institute for Biogeochemistry, Jena, Germany; Carrara—CEAM, Fundación de la Comunidad Valenciana Centro de Estudios Ambientales del Mediterraneo, Paterna, Spain; Kaminski and Vossbeck—The Inversion Lab, Hamburg, Germany; Otto—Environmental Change Institute, University of Oxford, Oxford, United Kingdom; Thonicke—Potsdam Institute for Climate Impact Research, Potsdam, Germany

DOI:10.1175/BAMS-D-17-0135.1

A supplement to this article is available online (10.1175/BAMS-D-17-0135.2)

While long-term climatic changes impose fundamental impacts on terrestrial ecosystems (Parmesan and Yohe 2003; Walther et al. 2002), cause–effect chains under climatic extremes are often highly nonlinear (Frank et al. 2015) and typically include instantaneous and lagged effects (Arnone et al. 2008). Ecosystem responses to climate extremes are specific to the ecosystem type affected (Teuling et al. 2010), depend on nutrient status, ecosystem health, and pre-exposure; and extreme climatic events can lead to little ecosystem responses while moderate events can trigger large responses. Similarly, ecosystem responses can be mitigated or amplified across seasons (Wolf et al. 2016). For example, higher spring carbon uptake due to higher spring temperatures could compensate for carbon losses under drought conditions over the contiguous United States in summer 2012 (Wolf et al. 2016).

To improve our understanding of extreme responses of ecosystem productivity, the concept of compound events is particularly useful. A compound event is a combination, or in our case succession, of events in which the single drivers are not necessarily extreme themselves but lead to an extreme impact (Field et al. 2012; Leonard et al. 2014). A warm winter followed by wet spring in a Mediterranean ecosystem is one example of a compound event in which single drivers (winter temperature and spring precipitation) are not record-breaking extremes themselves, but this favorable combination of meteorological variables can lead to highly positive impacts on ecosystem productivity if other stressors are absent. In particular, for the ecosystem studied, other stressors could include, but are not limited to, short but intense cold spells in

*S.S. and T.S.E.-M contributed equally to the manuscript.

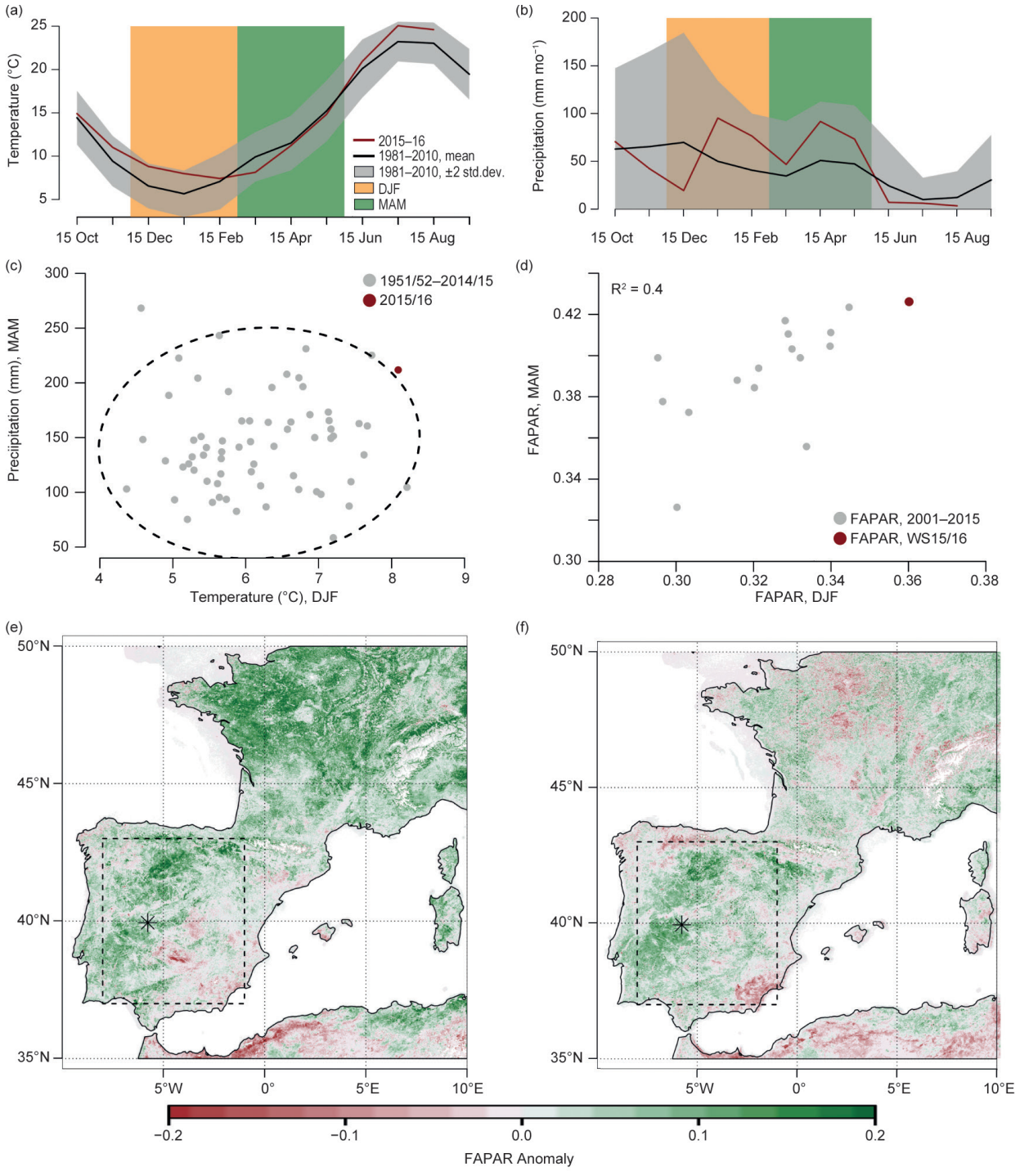

Fig. 16.1. (a),(b) Time series of (a) temperature (°C) and (b) precipitation (mm month^{-1}) over IP in 2015/16 (gray shading indicates ±2σ range, w.r.t. 1981–2010). (c),(d) Scatter plot of (c) winter temperature (°C) and spring precipitation (mm month^{-1}), and (d) winter and spring fraction of FAPAR. Ellipse denotes quantile of 95% in multivariate normal distribution (Santos-Fernández 2012). (e),(f) Map of relative anomaly in FAPAR in (e) winter and (f) spring 2015/16 w.r.t. 2001–16 (black dot indicates study site Majadas del Tietar; rectangle denotes model domain).

winter, moisture stress carried over from previous seasons, fires, pests, or legacy effects thereof.

In this paper, we: 1) analyze the extreme ecosystem productivity anomaly of WS15/16 at the regional scale

and with site-level measurements, including a process interpretation, and 2) assess, based on an ensemble of process-oriented ecosystem model simulations, how the odds of extremely positive vegetation productivity events [measured in gross primary productivity (GPP) and net ecosystem productivity (NEP)] in winter and spring are changing in response to climate change.

Winter 2015/16 and spring 2016: Meteorological drivers and extreme ecosystem impacts.

a. Regional-scale analysis of vegetation productivity. Strong and persistent anticyclonic conditions prevailed from November to mid-January over the Mediterranean basin, leading to the advection of very mild air into the IP and, in fact, into large parts of western Europe. For example, December 2015 was among the warmest months ever recorded in a range of European countries, such as Spain (2nd; Fig. 16.1a; www.aemet.es/documentos/es/serviciosclimaticos/vigilancia_clima/resumenes_climat/mensuales/2015/res_mens_clim_2015_12.pdf), France (1st; http://actualite.lachainemeteo.com/actualite-meteo/2015-12-26-06h09/decembre-2015---historiquement-chaud-et-sec-29466.php), and Germany (1st; www.dwd.de/DE/presse/pressemitteilungen/DE/2015/20151230_deutschlandwetter_dezember_news.html), among others; and combined December and January temperatures exceeded the previous IP area-average record value by 0.72°C in the EOBS—dataset (Haylock et al. 2008). In late winter, however, the synoptic situation changed with temperatures returning to near normal, and abundant above-average precipitation over the IP continuing from January through May (Fig. 16.1c). Hence, high winter temperatures were followed by high late winter and spring precipitation, exceeding a bivariate 95th percentile (Fig. 16.1c; see online supplement for details).

Continuously high temperatures during winter enable better functioning of plant enzymes used in the photosynthetic machinery (Sage and Kubien 2007) and prevent plants from damage through cold stress. The availability of water during spring prevents soils from drying out and the plants from experiencing drought stress. The 2015/16 meteorological conditions thus provided the basis for the highest area averaged IP fraction of absorbed photosynthetically active radiation (FAPAR, a proxy for ecosystem productivity observed from space that is related to the state and greenness of vegetation canopies; Gobron et al. 2010) in both winter and spring (Fig. 16.1d), using the Tip–FAPAR dataset (Pinty et al. 2011) in the MODIS era (2001–16); and positive FAPAR anomalies prevailed in both seasons across most of the IP except its southeastern parts (Figs. 16.1e,f).

A correlation analysis of concurrent and lagged meteorological variables and FAPAR at the seasonal time scale shows that IP FAPAR (as a regional-scale ecosystem productivity proxy) is mainly temperature-limited in winter, which gradually transcends toward water limitation in spring (Table ES16.1). While we focus only on the individual 2015/16 event, in fact out of the four years (i.e., 25% of the 16-year FAPAR record) that showed the highest December–May IP FAPAR, all four years were among the warmest 30% of IP winters in the EOBS—dataset, and three out of four among the wettest 30% of IP springs (and all four within the wettest 35% of springs on record). Nonetheless, FAPAR in IP ecosystems is also sensitive to precipitation in the previous season both in winter and spring (Table ES16.1), which highlights the role of lagged effects. Hence, the dependence on contemporaneous meteorological conditions should not be mistaken as the sole driver of positive ecosystem productivity events.

b. Site-scale analysis of vegetation productivity. In Spain, 2.16 million hectares of the vegetation used for livestock production consists of a mosaic of at least 20% oak woodlands plus grass- and shrublands, so-called dehesas. Over a quarter of this vegetation type is located in Extremadura (Campos et al. 2013) in which the study site, Majadas del Tietar (39.9415°N, –5.7734°E), is located (Casals et al. 2009).

The site was established in 2003 with meteorological measurements and eddy covariance flux measurements of energy, water vapor, and carbon dioxide, thus a 13-year record is available for analysis.

At site-level, the meteorological variables largely mirrored the regional-scale patterns, that is high temperatures in winter (2.5°C above site average in winter) and wet conditions in spring [57 mm (~25%) above site average precipitation in spring]. During the warm winter and wet spring, GPP exceeded the respective seasonal averages by 29 grams of carbon (gC) m^{-2} $month^{-1}$ (~45%) and 43 gC m^{-2} $month^{-1}$ (~30%). In addition, ecosystem respiration (Reco, the release of carbon by the ecosystem), is coupled to temperature and also increased during the warm winter by 29 gC m^{-2} $month^{-1}$ (70%) as compared to the average winter. The absence of water stress during the wet spring 2016 also led to increased Reco by 40 gC m^{-2} $month^{-1}$ (42%; Fig. ES16.1). Therefore, despite the fact that ecosystem productivity was high in WS15/16 as measured by FAPAR (Figs. 16.1e,f; Pearson correlation between FAPAR and $GPP_{site,}$ $R_{Dec\text{-}May} = 0.84$), the

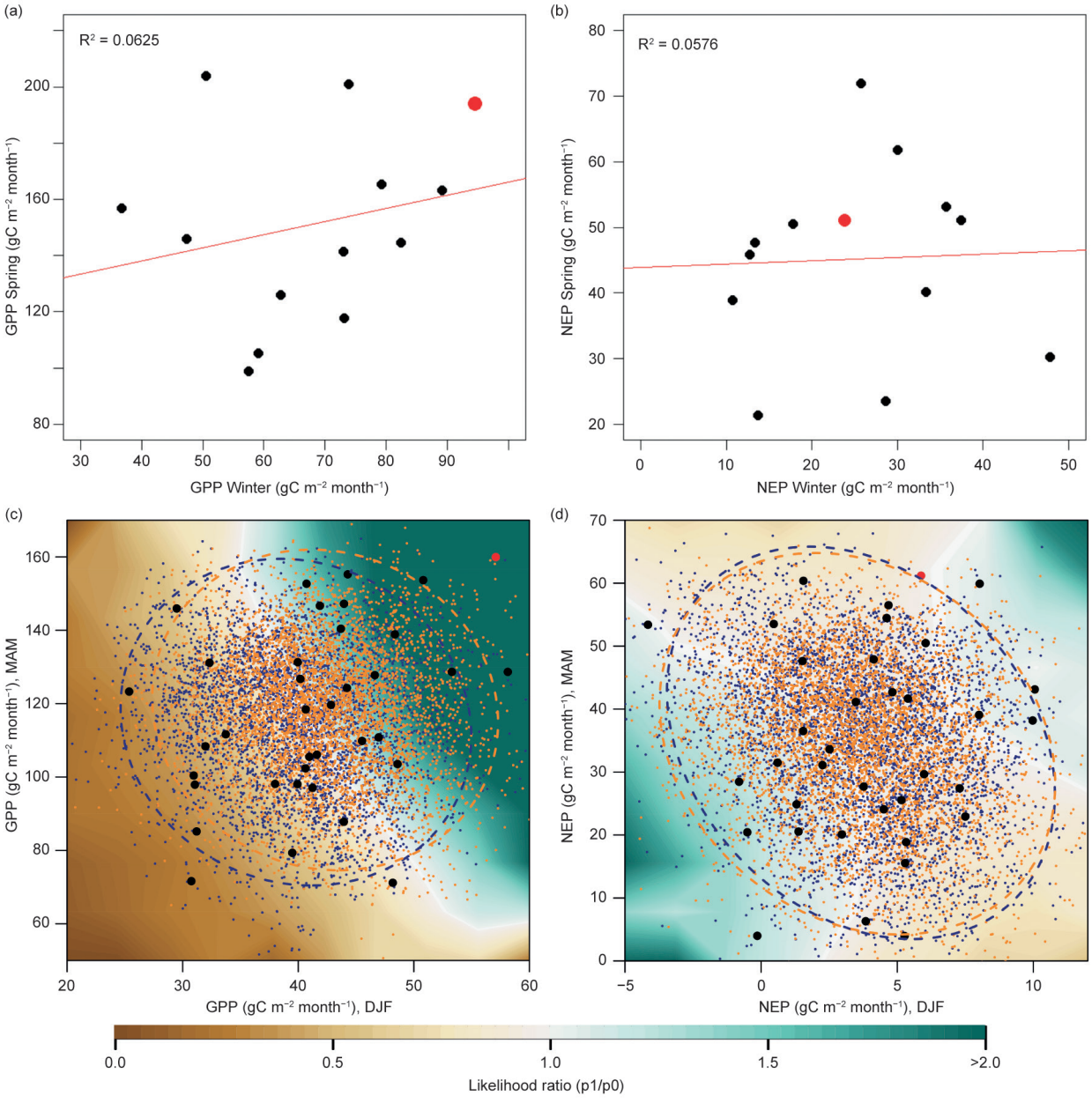

Fig. 16.2. (a) GPP and (b) NEP in winter and spring 2015/16 at Majadas del Tietar w.r.t. earlier years. (c),(d) Area-averaged ensemble ecosystem model simulations over the IP for (c) GPP and (d) NEP for earlier (1986–95, blue dots) and more recent (2001–10, orange dots) period; ellipses indicate bivariate 95% quantile. Black dots indicate LPJmL simulations driven by ERA-Interim for 1979–2015 (means adjusted); red dot is 2016. Background colors illustrate relative changes in event occurrence probabilities between earlier and more recent period (i.e., PR = p_{recent}/p_{early}) derived from multivariate normal distribution fitted to both model simulation periods individually. Units for GPP and NEP are gC m^{-2} month^{-1}.

simultaneous increase of GPP and Reco meant that NEP (the net sequestration of carbon) was not unusually high (Fig. 16.2b). This means, that an increase in ecosystem productivity does not necessarily lead to the ecosystem functioning as a larger carbon sink.

How do climatic changes affect regional-scale ecosystem productivity extremes? We provide an estimate of changes in the likelihood of ecosystem productivity extremes such as in 2015/16 based on a process-oriented ecosystem model over the time period of 1986–2010. To do so, we evaluate an ensemble of process-oriented ecosystem model simulations over

the IP (500 members in each year in 1986–2010), using the Lund–Potsdam–Jena managed Land (LPJmL) ecosystem model (Bondeau et al. 2007; Sitch et al. 2003). The simulations are driven by (i) a bias corrected regional climate model ensemble (Massey et al. 2015), and (ii) ERA-Interim reanalysis data (Dee et al. 2011) as a transient simulation reflecting observed meteorology (Pearson correlation between FAPAR and $GPP_{LPJmL-ERAI}$, $R_{Dec-May} = 0.83$). Further, the ecosystem model is run in two setups, that is, in standard mode with transient (i.e., observed) CO_2 concentrations, and a second setup with CO_2 values held constant at 1986 values ($CONSTCO_2$) in order to isolate direct CO_2 effects on ecosystem functioning. The climate model is driven by observed sea surface temperatures in the *weather@home* setup (Massey et al. 2015). A detailed methodological description of the HadRM3P–LPJmL ensemble approach is available in Sippel et al. (2017) and is summarized in the online supplement.

Overall, the ecosystem model simulations driven by ERA-Interim indicate that 2015/16 had been an extreme event in regional-scale GPP consistent with site-scale measurements (Fig. 16.2c), and to a lesser degree in NEP (Fig. 16.2d), which differs from site observations that do not indicate anomalous conditions. Contrasting the bivariate distribution of an earlier (1986–95) and a more recent period (2001–10) reveals that the odds for high winter GPP associated with high spring GPP have indeed increased, and the model indicates that the odds for an event similar to 2015/16 have more than doubled (Fig. 16.2c). These changes can be attributed to higher winter temperatures, consistent with anthropogenic climate change, in combination with CO_2 fertilization effects in the ecosystem model. Long-term meteorological observations show a strong trend in winter temperatures over the IP (Fig. ES16.2), which is reproduced by the climate model that drives the ecosystem model (both for the 2001–10 vs. 1986–95 decade, but also if the 2001–10 decade is compared to a hypothetical preindustrial 2001–10 ensemble; see Fig. ES16.2 and online supplement text for details). In contrast, there is no significant trend in IP spring precipitation neither in observations nor in the climate model (Fig. ES16.2). Thus increased odds for high spring GPP events that follow high winter GPP events (Fig. 16.2c) cannot be attributed to changes in spring precipitation. Instead, the increased odds in high spring GPP events arise from direct CO_2 effects in the ecosystem model, because these changes disappear in the $CONSTCO_2$ scenario (cf. Fig. ES16.3 and Fig. 16.2c). However, crucially, the ecosystem model ensemble simulations also indicate that net ecosystem carbon sequestration, that is after ecosystem respiration is accounted for, has not increased (Fig. 16.2d). This might be due to the fact that higher temperatures are associated with increased Reco (as consistently observed at site scale in Majadas in 2015/16).

Conclusion. Our study shows that the 2015/16 positive GPP anomaly on the Iberian Peninsula, which was enabled by a compound warm winter and wet spring event, is indeed consistent with recent observed climate change, as diagnosed in site and regional scale observations and model simulations. While the increase in winter GPP can be attributed to increasing temperatures, the increase in spring GPP cannot be attributed to changes in spring precipitation, but these changes result from increased CO_2 fertilization. However, these warming and CO_2-induced effects are largely canceled in terms of net ecosystem carbon sequestration in 2015/16, as carbon uptake and release intensified in tandem, which is consistent with expectations in a changing climate as indicated by the ecosystem model ensemble. This study presents and discusses a novel inquiry into the attribution of ecosystem impacts to extreme climate events and the underlying drivers. However, because it uses only one combination of climate–ecosystem models, and a relatively short observational record, its conclusions should be regarded as contingent on these limitations.

ACKNOWLEDGMENTS. S. S., M. D. M., and M. F. thank the European Space Agency for funding the STSE project CAB-LAB. T. S. E.-M., M. M. and M. R. thank the Alexander von Humboldt Foundation for supporting this research with the Max Planck Research Award to Markus Reichstein. We thank the two reviewers and the editor for their valuable comments and ideas to enhance the quality of this manuscript.

REFERENCES

Arnone, J. A., and Coauthors, 2008: Prolonged suppression of ecosystem carbon dioxide uptake after an anomalously warm year. *Nature*, **455**, 383–386, doi:10.1038/nature07296.

Bondeau, A., and Coauthors, 2007: Modelling the role of agriculture for the 20th century global terrestrial carbon balance. *Global Change Biol.*, **13**, 679–706, doi: 10.1111/j.1365-2486.2006.01305.x.

Campos, P., L. Huntsinger, J. L. Oviedo, P. F. Starrs, M. Díaz, R. B. Standiford, and G. Montero, Eds., 2013: *Mediterranean Oak Woodland Working Landscapes*. Landscape Series, Vol. 16, Springer, 508 pp.

Casals, P., C. Gimeno, A. Carrara, L. Lopez-Sangil, and M. J. Sanz, 2009: Soil CO_2 efflux and extractable organic carbon fractions under simulated precipitation events in a Mediterranean Dehesa. *Soil Biol. Biochem.*, **41**, 1915–1922, doi:10.1016/j.soilbio.2009.06.015.

Dee, D. P., and Coauthors, 2011: The ERA-Interim reanalysis: configuration and performance of the data assimilation system. *Quart. J. Roy. Meteor. Soc.*, **137,** 553–597, doi:10.1002/qj.828.

Field, C. B., and Coauthors, Eds., 2012: *Managing the Risks of Extreme Events and Disasters to Advance Climate Change Adaptation*. Cambridge University Press, 582 pp. [Available online at www.ipcc-wg2.gov/SREX/images/uploads/SREX-All_FINAL.pdf.]

Frank, D. A., and Coauthors, 2015: Effects of climate extremes on the terrestrial carbon cycle: Concepts, processes and potential future impacts. *Global Change Biol.*, **21**, 2861–2880, doi:10.1111/gcb.12916.

Gobron, N., A. Belward, B. Pinty, and W. Knorr, 2010: Monitoring biosphere vegetation 1998–2009. *Geophys. Res. Lett.*, **37**, L15402, doi:10.1029/2010GL043870.

Haylock, M. R., N. Hofstra, A. M. G. K. Tank, E. J. Klok, P. D. Jones, and M. New, 2008: A European daily high-resolution gridded data set of surface temperature and precipitation for 1950–2006. *J. Geophys. Res.*, **113**, D20119, doi:10.1029/2008JD010201.

Leonard, M., and Coauthors, 2014: A compound event framework for understanding extreme impacts. *Wiley Interdiscip. Rev.: Climate Change*, **5**, 113–128, doi:10.1002/wcc.252.

Massey, N., and Coauthors, 2015: weather@ home—development and validation of a very large ensemble modelling system for probabilistic event attribution. *Quart. J. Roy. Meteor. Soc.*, **141**, 1528–1545, doi:10.1002/qj.2455.

Parmesan, C., and G. Yohe, 2003: A globally coherent fingerprint of climate change impacts across natural systems. *Nature*, **421**, 37–42, doi:10.1038/nature01286.

Pinty, B., and Coauthors, 2011: Exploiting the MODIS albedos with the Two-stream Inversion Package (JRC-TIP): 2. Fractions of transmitted and absorbed fluxes in the vegetation and soil layers. *J. Geophys. Res.*, **116**, D09106, doi:10.1029/2010JD015373.

Reichstein, M., and Coauthors, 2013: Climate extremes and the carbon cycle. *Nature*, **500**, 287–295, doi:10.1038/nature12350.

Sage, R. F., and D. S. Kubien, 2007: The temperature response of C_3 and C_4 photosynthesis. *Plant, Cell Environ.*, **30,** 1086–1106, doi:10.1111/j.1365-3040.2007.01682.x.

Santos-Fernández, E., 2012: *Multivariate Statistical Quality Control Using R*. SpringerBriefs in Statistics, Vol. 14, Springer, 127 pp.

Seneviratne, S. I., and Coauthors, 2012: Changes in climate extremes and their impacts on the natural physical environment. *Managing the Risks of Extreme Events and Disasters to Advance Climate Change Adaptation,* C. B. Field et al., Eds., Cambridge Univeristy Press, 109–230.

Sippel, S., and Coauthors, 2017: Contrasting and interacting changes in simulated spring and summer carbon cycle extremes in European ecosystems. *Environ. Res. Lett.*, **12**, 075006, doi:10.1088/1748-9326/aa7398.

Sitch, S., and Coauthors, 2003: Evaluation of ecosystem dynamics, plant geography and terrestrial carbon cycling in the LPJ dynamic global vegetation model. *Global Change Biol.*, **9**, 161–185.

Teuling, A. J., and Coauthors, 2010: Contrasting response of European forest and grassland energy exchange to heatwaves. *Nat. Geosci.*, **3**, 722–727, doi:10.1038/ngeo950.

Walther, G. R., and Coauthors, 2002: Ecological responses to recent climate change. *Nature*, **416**, 389–395, doi:10.1038/416389a.

Wolf, S., and Coauthors, 2016: Warm spring reduced carbon cycle impact of the 2012 US summer drought. *Proc. Natl. Acad. Sci. USA*, **113**, 5880–5885, doi:10.1073/pnas.1519620113.

Table 1.1. SUMMARY of RESULTS

ANTHROPOGENIC INFLUENCE ON EVENT			
	INCREASE	**DECREASE**	**NOT FOUND OR UNCERTAIN**
Heat	Ch. 3: Global Ch. 7: Arctic Ch. 15: France Ch. 19: Asia		
Cold		Ch. 23: China Ch. 24: China	
Heat & Dryness	Ch. 25: Thailand		
Marine Heat	Ch. 4: Central Equatorial Pacific Ch. 5: Central Equatorial Pacific Ch. 6: Pacific Northwest Ch. 8: North Pacific Ocean/Alaska Ch. 9: North Pacific Ocean/Alaska Ch. 9: Australia		Ch. 4: Eastern Equatorial Pacific
Heavy Precipitation	Ch. 20: South China Ch. 21: China (Wuhan) Ch. 22: China (Yangtze River)		Ch. 10: California (failed rains) Ch. 26: Australia Ch. 27: Australia
Frost	Ch. 29: Australia		
Winter Storm			Ch. 11: Mid-Atlantic U.S. Storm "Jonas"
Drought	Ch. 17: Southern Africa Ch. 18: Southern Africa		Ch. 13: Brazil
Atmospheric Circulation			Ch. 15: Europe
Stagnant Air			Ch. 14: Western Europe
Wildfires	Ch. 12: Canada & Australia (Vapor Pressure Deficits)		
Coral Bleaching	Ch. 5: Central Equatorial Pacific Ch. 28: Great Barrier Reef		
Ecosystem Function		Ch. 5: Central Equatorial Pacific (Chl-***a*** and primary production, sea bird abundance, reef fish abundance) Ch. 18: Southern Africa (Crop Yields)	
El Niño	Ch. 18: Southern Africa		Ch. 4: Equatorial Pacific (Amplitude)
TOTAL	18	3	9

	METHOD USED	Total Events
Heat	Ch. 3: CMIP5 multimodel coupled model assessment with piCont, historicalNat, and historical forcings Ch. 7: CMIP5 multimodel coupled model assessment with piCont, historicalNat, and historical forcings Ch. 15: Flow analogues conditional on circulation types Ch. 19: MIROC-AGCM atmosphere only model conditioned on SST patterns	
Cold	Ch. 23: HadGEM3-A (GA6) atmosphere only model conditioned on SST and SIC for 2016 and data fitted to GEV distribution Ch. 24: CMIP5 multimodel coupled model assessment	
Heat & Dryness	Ch. 25: HadGEM3-A N216 Atmosphere only model conditioned on SST patterns	
Marine Heat	Ch. 4: SST observations; SGS and GEV distributions; modeling with LIM and CGCMs (NCAR CESM-LE and GFDL FLOR-FA) Ch. 5: Observational extrapolation (OISST, HadISST, ERSST v4) Ch. 6: Observational extrapolation; CMIP5 multimodel coupled model assessment Ch. 8: Observational extrapolation; CMIP5 multimodel coupled model assessment Ch. 9: Observational extrapolation; CMIP5 multimodel coupled model assessment	
Heavy Precipitation	Ch. 10: CAM5 AMIP atmosphere only model conditioned on SST patterns and CESM1 CMIP single coupled model assessment Ch. 20: Observational extrapolation; CMIP5 and CESM multimodel coupled model assessment; auto-regressive models Ch. 21: Observational extrapolation; HadGEM3-A atmosphere only model conditioned on SST patterns; CMIP5 multimodel coupled model assessment with ROF Ch. 22: Observational extrapolation, CMIP5 multimodel coupled model assessment Ch. 26: BoM seasonal forecast attribution system and seasonal forecasts Ch. 27: CMIP5 multimodel coupled model assessment	
Frost	Ch. 29: *weather@home* multimodel atmosphere only models conditioned on SST patterns; BoM seasonal forecast attribution system	
Winter Storm	Ch. 11: ECHAM5 atmosphere only model conditioned on SST patterns	
Drought	Ch. 13: Observational extrapolation; weather@home multimodel atmosphere only models conditioned on SST patterns; HadGEM3-A and CMIP5 multimodel coupled model assessent; hydrological modeling Ch. 17: Observational extrapolation; CMIP5 multimodel coupled model assessment; VIC land surface hdyrological model, optimal fingerprint method Ch. 18: Observational extrapolation; *weather@home* multimodel atmosphere only models conditioned on SSTs, CMIP5 multimodel coupled model assessment	
Atmospheric Circulation	Ch. 15: Flow analogues distances analysis conditioned on circulation types	
Stagnant Air	Ch. 14: Observational extrapolation; Multimodel atmosphere only models conditioned on SST patterns including: HadGEM3-A model; EURO-CORDEX ensemble; EC-EARTH+RACMO ensemble	
Wildfires	Ch. 12: HadAM3 atmospere only model conditioned on SSTs and SIC for 2015/16	
Coral Bleaching	Ch. 5: Observations from NOAA Pacific Reef Assessment and Monitoring Program surveys Ch. 28: CMIP5 multimodel coupled model assessment; Observations of climatic and environmental conditions (NASA GES DISC, HadCRUT4, NOAA OISSTV2)	
Ecosystem Function	Ch. 5: Observations of reef fish from NOAA Pacific Reef Assessment and Monitoring Program surveys; visual observations of seabirds from USFWS surveys. Ch. 18: Empirical yield/rainfall model	
El Niño	Ch. 4: SST observations; SGS and GEV distributions; modeling with LIM and CGCMs (NCAR CESM-LE and GFDL FLOR-FA) Ch. 18: Observational extrapolation; *weather@home* multimodel atmosphere only models conditioned on SSTs, CMIP5 multimodel coupled model assessment	
		30